Journal of Magnetism and Magnetic Materials 335 (2013) 172–176

Contents lists available at SciVerse ScienceDirect

Journal of Magnetism and Magnetic Materials

journal homepage: www.elsevier.com/locate/jmmm

Magnetic properties of $(Fe_{1-x}Ni_x)_{72}B_{20}Si_4Nb_4$ ($x=0.0$–0.5) bulk metallic glasses

Weiming Yang [a,b], Haishun Liu [a,*], Lin Xue [a,b], Jiawei Li [b], Chaochao Dun [a], Jianhua Zhang [b], Yucheng Zhao [a], Baolong Shen [c,**]

[a] School of Mechanics and Civil Engineering, School of Sciences, China University of Mining and Technology, Xuzhou 221116, China
[b] Zhejiang Province Key Laboratory of Magnetic Materials and Application Technology, Key Laboratory of Magnetic Materials and Devices, Ningbo Institute of Materials Technology & Engineering, Chinese Academy of Sciences, Ningbo 315201, China
[c] School of Materials Science and Engineering, Southeast University, Nanjing 211189, China

ARTICLE INFO

Article history:
Received 8 October 2012
Received in revised form
22 January 2013
Available online 11 February 2013

Keywords:
Bulk metallic glass
Saturation polarization
Curie temperature

ABSTRACT

The effects of partial substitution of Fe by Ni in $(Fe_{1-x}Ni_x)_{72}B_{20}Si_4Nb_4$ ($x=0.0$, 0.1, 0.2, 0.3, 0.4, and 0.5) bulk metallic glasses (BMGs) on their magnetic properties were studied. It is found that the saturation polarization decreases from 1.15 T to 0.69 T with increasing Ni content from $x=0.0$ to $x=0.5$; the Curie temperature reaches its maximum of 598 K for composition $x=0.1$, and is then followed by a quick decrease with higher Ni content. Moreover, the random anisotropy and mean field theory were developed to investigate the magnetic properties of these BMGs, and the variations of saturation polarization and Curie temperature were well explained by calculating the magnetic exchange stiffness constant A and the nearest neighbor transition-metal-pair exchange interactions J by using the model.

1. Introduction

Bulk metallic glasses (BMGs) have attracted great attention due to their unique properties and potential applications [1–3]. Among them, the Fe-based BMGs are more attractive for application since they not only possess many good properties, such as excellent soft magnetic properties [4,5], besides ultrahigh strength [6–8] and good anticorrosion property [9], but are also much cheaper in comparison to other BMGs [10]. Recently, Fe-based BMGs have been intensively investigated and their critical size has been increased [11–16]. It is found that partial substitution of Fe with other magnetic elements Ni or Co may remarkably enhance the GFA [17,18] and change the soft magnetic properties due to compositional variation [19,20]; nevertheless, it is also found that the effects of Ni and Co on magnetic properties are somewhat different from each other [21,22], even if they are at neighboring positions in the Element Periodic Table. However, little attention concerning how and why the magnetic properties change induced by partial substitution of Fe by Ni was paid, and even less detailed theoretical research on the mechanism of partial substitution of Fe with constituting elements in Fe-based BMGs was carried out.

In the present work, we investigated the effects of partial substitution of Fe by Ni on the thermal characteristics and magnetic properties of Fe–B–Si–Nb BMGs considering its high GFA and excellent magnetic properties [12,18]. On this basis, the random anisotropy and mean field theory of the magnetic properties for $(Fe_{1-x}Ni_x)_{72}B_{20}Si_4Nb_4$ ($x=0.0$, 0.1, 0.2, 0.3, 0.4, and 0.5) were developed to explain the variations of saturation polarization and Curie temperature.

2. Experiments

Multi-component $(Fe_{1-x}Ni_x)_{72}B_{20}Si_4Nb_4$ ($x=0.0$, 0.1, 0.2, 0.3, 0.4, and 0.5) ingots were prepared by arc melting the mixtures of Fe (99.99%), Ni (99.99%) and Nb (99.99%) metals, and B (99.5%) and Si (99.999%) crystals in an argon atmosphere. Cylindrical alloy rods with diameters of 1.5 mm were produced by the copper mold casting method. The structures of as-cast samples were identified by X-ray diffraction (XRD) with Cu Kα radiation. The thermal stability of the glassy samples was examined using a NETZSCH 404 C differential scanning calorimeter (DSC) at a heating rate of 0.67 K/s under a flow of high purity argon. The Curie temperature of the as-cast alloys was measured by a physical property measurement system (PPMS) at a heating rate of 0.167 K/s. For magnetic properties investigation, M–H hysteresis loops were measured with a vibrating sample magnetometer (VSM) at ambient temperatures. Additionally, the density of the specimens was measured using Archimedes's method with the accuracy less than 1%.

* Corresponding author. Tel.: +86 139 12006872; fax: +86 516 83591591.
** Corresponding author. Tel.: +86 25 52091077; fax: +86 25 52090669.
E-mail addresses: liuhaishun@126.com (H. Liu), blshen@seu.edu.cn (B. Shen).

0304-8853/$ - see front matter © 2013 Elsevier B.V. All rights reserved.
http://dx.doi.org/10.1016/j.jmmm.2013.02.004

3. Results and discussion

Fig. 1 shows the XRD patterns for all six as-cast rods with diameter of 1.5 mm. It can be seen that each pattern contains only broad maxima without any additional sharp Bragg peaks, and the diffraction images did not show any traces of crystallinity. This is characteristic of fully amorphous samples. It is found that as the content of Ni increases, the diffraction angle of the principal diffuse peak in XRD pattern is almost unchanged. The position of an X-ray halo maximum is known to be directly related to the average radius of the first coordination shell, r_1, according to the Bragg equation: $2r_1 \sin\theta = \lambda$ with λ the X-ray wavelength and 2θ the scatter angle corresponding to the halo maximum. The almost unchanged first peak might be due to the almost equal radius of Ni (0.125 nm) and Fe (0.124 nm) [23]; even if Fe was replaced by Ni, the value of r_1 remains almost unchanged, which leads to nearly invariant 2θ.

Fig. 2(a) presents the DSC traces of the as-cast $(Fe_{1-x}Ni_x)_{72}B_{20}Si_4Nb_4$ (x=0.0, 0.1, 0.2, 0.3, 0.4, and 0.5) BMGs measured at a constant heating rate of 0.67 K/s. It can be seen that all DSCs exhibit one endothermic event characteristic of the glass transition from the amorphous solid to the supercooled, followed by a crystallization exothermic reaction, which further confirms the glassy nature of the rods. Although T_g and T_x decrease from 837 to 776 K and from 882 to 834 K, respectively, ΔT_x increases gradually from 45 to 58 K with increasing Ni content to x=0.5. Thus, it is suggested that the thermal stability of the supercooled liquid increases with increasing Ni. Fig. 2(b) describes DSC curves revealing the cooling behavior of the same Fe-based BMGs system, which demonstrates that the $Fe_{72}B_{20}Si_4Nb_4$ BMG exhibits the highest T_l and T_e of 1479 and 1405 K, respectively, as well as the largest temperature interval ($T_l - T_e$) of 74 K, implying that this composition does not lie in the vicinity of a eutectic point. With increasing Ni content from x=0.1 to x=0.5, the T_l and T_e decrease gradually from 1471 to 1298 K and from 1405 to 1291 K, respectively, indicating that the alloy approaches a eutectic point in this process; especially when x=0.4, T_l is very close to T_e; thus, it is considered to be the closest to the eutectic point in this alloy system.

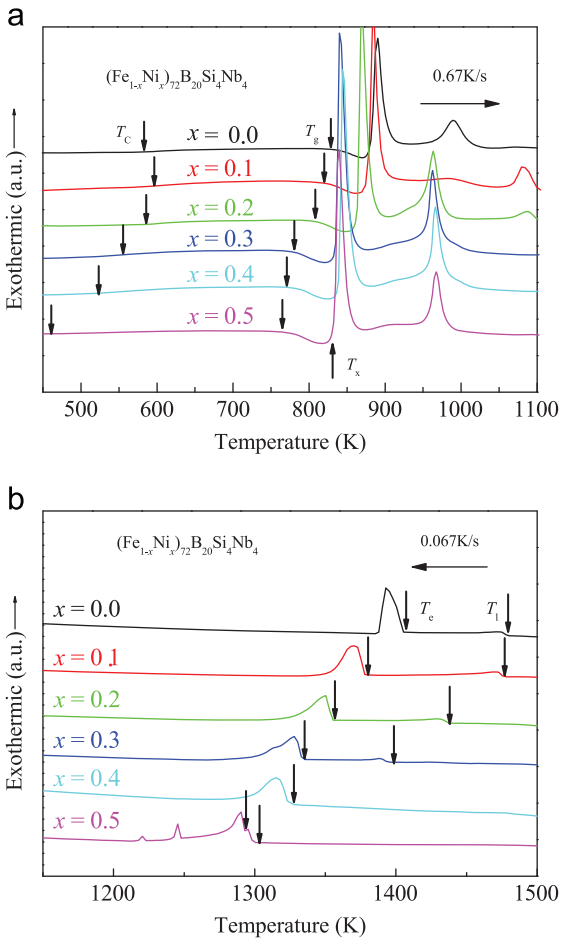

Fig. 2. (a) DSC traces measured at a constant heating rate of 0.67 K/s for cast $(Fe_{1-x}Ni_x)_{72}B_{20}Si_4Nb_4$ (x=0.0, 0.1, 0.2, 0.3, 0.4, and 0.5) alloys. (b) DSC traces measured at a constant cooling rate of 0.067 K/s for cast $(Fe_{1-x}Ni_x)_{72}B_{20}Si_4Nb_4$ (x=0.0, 0.1, 0.2, 0.3, 0.4, and 0.5) alloys.

3.1. Saturation polarization

As expected, the fully glassy samples display excellent magnetic properties. Table 1 summarizes the saturation magnetization M_S (given in Am^2/kg and in Bohr magnetons μ_B per magnetic atom), saturation polarization J_S and Curie temperature T_C as well as the density ρ for as-cast samples. Here, the saturation polarization was calculated by using the actual density values ($J_S = 4\pi \times 10^{-7} \rho M_S$), as presented in Fig. 3, and the saturation polarization as a function of Ni content is shown in Fig. 4. We can see that the saturation polarization decreases monotonically from 1.15 to 0.69 T upon increasing Ni content from x=0.0 to 0.5.

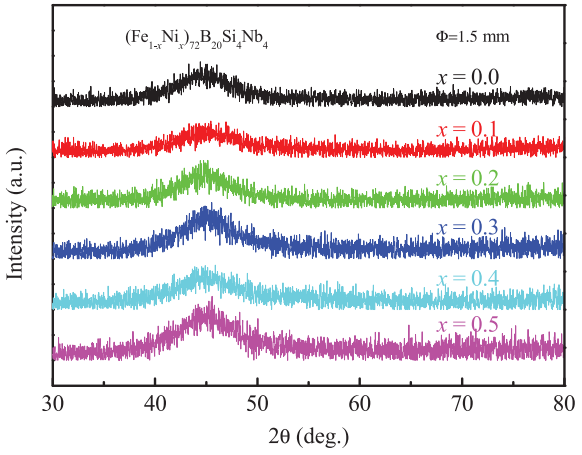

Fig. 1. XRD patterns of the cast $(Fe_{1-x}Ni_x)_{72}B_{20}Si_4Nb_4$ (x=0.0, 0.1, 0.2, 0.3, 0.4, and 0.5) alloys rods with diameters of 1.5 mm.

Table 1
Magnetic properties data for $(Fe_{1-x}Ni_x)_{72}B_{20}Si_4Nb_4$ glassy rods: magnetization at saturation M_S (given in A m^2/kg and in Bohr magnetons μ_B per magnetic atom), saturation polarization J_S, and Curie temperature T_C. Additionally, the density ρ is also shown.

Atomic fraction x	M_S (A m^2/kg)	J_S (T)	M_S (μ_B)	T_C (K)	ρ (g/cm^3)
0.0	123.2	1.15	1.25	581	7.4377
0.1	115.4	1.08	1.14	598	7.4493
0.2	104.9	0.99	1.05	588	7.4868
0.3	95.5	0.91	0.95	565	7.5794
0.4	81.6	0.78	0.81	525	7.6559
0.5	70.8	0.69	0.71	458	7.7576

The variation of saturation polarization as a function of Ni content should be explained in more detail. From the random anisotropy theory [24], the correlation between the saturation polarization and the exchange stiffness constant A can be expressed as

$$J_S = \frac{8 \times 10^{-7} \pi \rho A}{H_{ex} R_a^2} \quad (1)$$

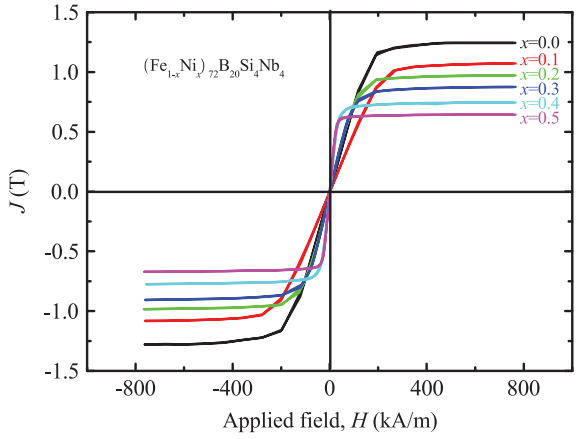

Fig. 3. DC hysteresis loops for cast $(Fe_{1-x}Ni_x)_{72}B_{20}Si_4Nb_4$ (x=0, 0.1, 0.2, 0.3, 0.4, and 0.5) glassy samples.

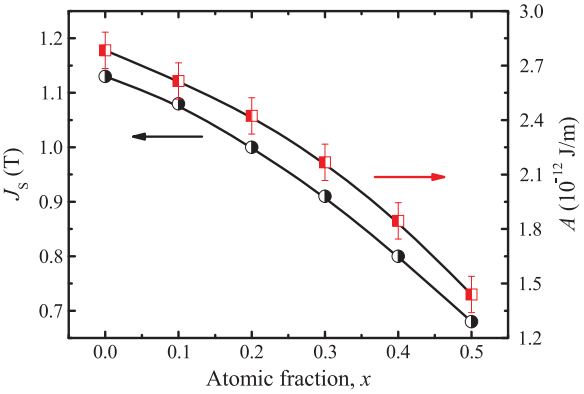

Fig. 4. Variations of saturation polarization and exchange stiffness constant A as a function of the atomic fraction x.

where H_{ex} is the exchange field which remains unchanged, R_a the length over which the local axes show a correlation (typically 10 é) [25], and ρ the density. Consequently, the saturation polarization J_s is proportional to the exchange stiffness constant A, and the latter can be obtained from the Curie temperature T_C. On the basis of Hasegawa's model, one can derive the following equation [26]:

$$A = \frac{x_{Fe}\, S_{Fe-Fe}\, k_B T_C}{4(S_{Fe-Fe}+1) r_{Fe-Fe}} \tag{2}$$

where x_{Fe} is the concentration of Fe in atomic percent, S_{Fe-Fe} the spin moment of Fe, T_C the Curie temperature, k_B the Boltzmann constant, and r_{Fe-Fe} the nearest-neighbor distance, which is considered to be twice the Fe atomic radius. Moreover, S_{Fe-Fe} can be calculated by

$$S_{Fe-Fe} = M(\mu_B)/2x_{Fe}\ \mu_B \tag{3}$$

in which $M(\mu_B)$ is the magnetic moment of the samples considering Bohr magnetons ($M(\mu_B)=J_S Z/\rho N_A$, and here Z is the molar mass). However, Eq. (3) is valid only when the starting alloy sample (x=0.0) or the Fe–Ni and Ni–Ni interactions could be ignored.

Normally, when Fe is partially substituted by Ni, the magnetic saturation should be considered as

$$M(\mu_B) = wM_{Fe}(\mu_B) + (1-w)M_{Ni}(\mu_B) \tag{4}$$

in which $M_{Fe}(\mu_B)$ and $M_{Ni}(\mu_B)$ are the magnetic moments of Ni-free and Fe-free amorphous alloys respectively, and w is the atomic fraction Fe/(Fe+Ni).

From the above analysis, the exchange stiffness constant A as a function of the atomic fraction x (the Ni content) was calculated, as shown in Fig. 4. It can be seen that the exchange stiffness constant A decreases from 2.73×10^{-12} J/m to 1.47×10^{-12} J/m when x increases from 0 to 0.5. The decrease of the stiffness constant means the promotion of the magnetic anisotropy and accordingly a decrease of exchange energy; as a result, the saturation magnetization decreases accordingly with increasing Ni content.

3.2. Curie temperature

Values of the T_C for various compositions of $(Fe_{1-x}Ni_x)_{72}B_{20}Si_4Nb_4$ BMGs are shown in Fig. 5. Fig. 5 presents a number of salient T_C going through a broad maximum at x=0.1 for the alloy series, which decreases rapidly as x increases. The corresponding values are also summarized in Table 1. Moreover, in order to confirm this phenomenon, the thermomagnetic curves, measured at a constant heating rate of 0.167 K/s up to 800 K, are presented in Fig. 6(a). Apparently, all the samples did not start to crystallize yet and the values correspond to the glassy states. The saturation magnetization can be described by $M_S(T)=M(0)(1-T/T_C)^{0.36}$ [20,27]. In order to minimize the errors, the experimental results were plotted as $M_S(T)^{0.36}$ vs T, shown in Fig. 6(b). It was considered that T_C deviates from linearity. We can see that the T_C measured by DSC is in agreement with that obtained from PPMS. The small deviation can be attributed to the experimental error. The T_C goes through a broad maximum at x=0.1 for Fe-rich alloys, indicating a large Fe–Fe exchange (J_{Fe-Fe}) which is ferromagnetic, whereas the sharp decrease in the values of T_C for the Ni-rich alloys suggests that the Ni–Ni exchange (J_{Ni-Ni}) tends to be weaker and weaker as Ni concentration increases. In order to arrive at a quantitative estimation of these exchange interactions, it is imperative to compare the experimentally observed dependence of T_C on x with theoretical models. It is obvious that the mean-field model can be used to explain the variation of T_C with x [28]. According to this theory, the calculation of T_C for two sublattices reduces to

$$T_C = \frac{1}{2}[T_{Ni-Ni}x + T_{Fe-Fe}(1-x)] + \left\{\frac{1}{4}[T_{Ni-Ni}x + T_{Fe-Fe}(1-x^2)]^2 + T^2_{Fe-Ni}x(1-x)\right\}^{1/2} \tag{5}$$

where

$$T_{Fe-Fe} = \frac{S_{Fe-Fe}(S_{Fe-Fe}+1)J_{Fe-Fe}}{3k_B}$$

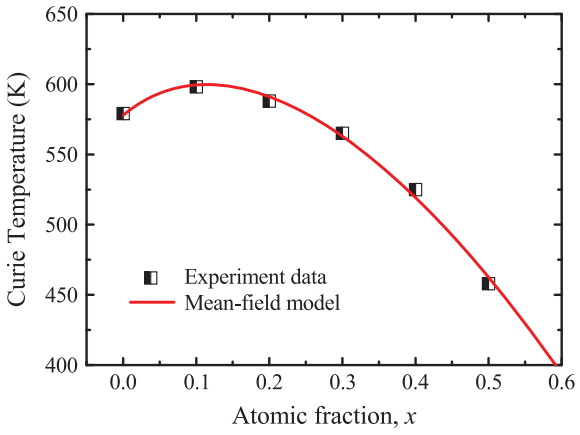

Fig. 5. Comparisons of experimental and theoretical data of Curie temperature for $(Fe_{1-x}Ni_x)_{72}B_{20}Si_4Nb_4$ as-cast glassy samples with the atomic fraction x.

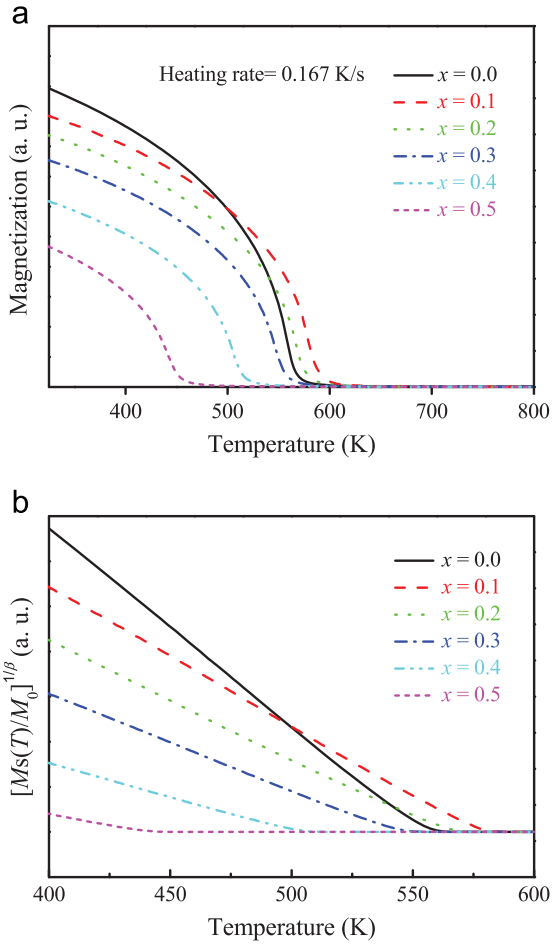

Fig. 6. (a) Thermomagnetic curves for as-cast $(Fe_{1-x}Ni_x)_{72}B_{20}Si_4Nb_4$ (x=0, 0.1, 0.2, 0.3, 0.4, and 0.5) glassy samples. (b) The relationship between $M_S(T)^{0.36}$ and T for as-cast $(Fe_{1-x}Ni_x)_{72}B_{20}Si_4Nb_4$ (x=0, 0.1, 0.2, 0.3, 0.4, and 0.5) glassy samples.

$$T_{Fe-Ni} = \frac{\sqrt{S_{Ni-Ni}S_{Fe-Fe}(S_{Ni-Ni}+1)(S_{Fe-Fe}+1)}J_{Fe-Ni}}{3k_B}$$

$$T_{Ni-Ni} = \frac{S_{Ni-Ni}(S_{Ni-Ni}+1)J_{Ni-Ni}}{3k_B}$$

where J_{ij} (i=Fe, j=Ni) is the exchange interaction. The experimental and corresponding theoretical calculations of T_C for $(Fe_{1-x}Ni_x)_{72}B_{20}Si_4Nb_4$ (x=0, 0.1, 0.2, 0.3, 0.4, and 0.5) alloys are shown in Fig. 5. We can clearly see that the fitting curves from our model are in good agreement with the experiments. Here, the parameters T_{Fe-Fe}, T_{Ni-Ni}, and T_{Fe-Ni} obtained from the fitting of experimental data by using Eq. (5) are 575 K, −318 K, and 754 K, respectively, which are in agreement with Ref. [29]. Moreover, the variation of the exchange interactions J_{ij} as a function of the atomic fraction x was also obtained, as shown in Fig. 7. It reveals that magnitude of both J_{Fe-Fe} and J_{Ni-Ni} decreases with increasing Ni concentration; however, the magnitude of J_{Fe-Ni} increases with increasing Ni. The total nearest neighbor transition-metal-pair exchange interactions can be expressed as

$$J = J_{Fe-Fe} + J_{Fe-Ni} + J_{Ni-Ni} \quad (6)$$

Thus, we can get that J goes through a broad maximum at x=0.1, and then decreases sharply as x increases, just as shown in Fig. 7, which demonstrates that the results can be explained by the present work.

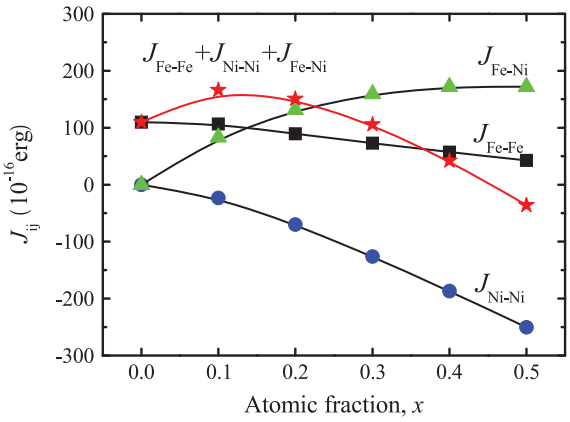

Fig. 7. Variation of the exchange interactions J_{ij} as a function of the atomic fraction x.

4. Conclusions

In this paper, the effects of substitution of Fe by Ni on magnetic properties of $(Fe_{1-x}Ni_x)_{72}B_{20}Si_4Nb_4$ BMGs with x=0.0, 0.1, 0.2, 0.3, 0.4, and 0.5 were studied. It is drawn that partial substitution of Fe by Ni results in the decreased saturation polarization and increased Curie temperature, but first goes through a maximum for x=0.1. The exchange stiffness constant calculated by the random anisotropy model follows the trend of experiments, and the exchange interaction shows a maximum at x=0.1 for Ni in the alloy from mean field theory.

Acknowledgments

We wish to thank Dr. C.T. Chang for technical assistance and discussions. The authors also wish to thank Dr. S.P. Pan and Y.W. Bai for their valuable discussions. This work was supported by the National Natural Science Foundation of China (Grant nos. 51074155, 50825103, 51271194 and 50834004), National Basic Research Program of China (2010CB226805) and Research Project funded by the Colleges and Universities in Jiangsu Province plans to graduate research and innovation (CXZZ12-0922).

References

[1] A.L. Greer, Science 267 (1995) 1947.
[2] H.Y. Zhang, R. Li, Y.F. Ji, F.M. Liu, Q. Luo, T. Zhang, Journal of Magnetism and Magnetic Materials 324 (2012) 4064.
[3] W.H. Wang, Nature Materials 11 (2012) 275.
[4] H.X. Li, H.Y. Jung, S. Yi, Journal of Magnetism and Magnetic Materials 320 (2008) 241.
[5] B.L. Shen, M. Akiba, A. Inoue, Applied Physics Letters 88 (2006) 131907.
[6] Z.F. Zhang, F.F. Wu, W. Gao, J. Tan, Z.G. Wang, M. Stoica, J. Das, J. Eckert, B.L. Shen, A. Inoue, Applied Physics Letters 89 (2006) 251917.
[7] J.H. Yao, J.Q. Wang, Y. Li, Applied Physics Letters 92 (2008) 251906.
[8] K.F. Yao, C.Q. Zhang, Applied Physics Letters 90 (2007) 061901.
[9] S.J. Pang, T. Zhang, K. Asami, A. Inoue, Acta Materialia 50 (2002) 489.
[10] Z.P. Lu, C.T. Liu, J.R. Thompson, W.D. Porter, Physical Review Letters 92 (2004) 2455031.
[11] A. Inoue, Acta Materialia 48 (2000) 279.
[12] K. Amiya, A. Urata, N. Nishiyama, A. Inoue, Materials Transactions 45 (2004) 1214.
[13] A. Inoue, B.L. Shen, Materials Transactions 43 (2002) 766.
[14] M. Stoica, R. Li, A.R. Yavari, G. Vaughan, J. Eckert, N.V. Steenberge, D.R. Romera, Journal of Alloys and Compounds 504S (2010) S123.
[15] Q. Li, J.F. Li, P. Gong, K.F. Yao, J.G. Gao, H.X. Li, Intermetallics 26 (2012) 62.
[16] W.M. Yang, H.S. Liu, C.C. Dun, J.W. Li, Y.C. Zhao, B.L. Shen, Journal of Non-Crystalline Solids 361 (2013) 82.
[17] C.T. Chang, B.L. Shen, A. Inoue, Applied Physics Letters 89 (2006) 051912.
[18] K. Amiya, A. Urata, N. Nishiyama, A. Inoue, Journal of Applied Physics 97 (2005) 10F913.
[19] C.T. Chang, B.L. Shen, A. Inoue, Applied Physics Letters 88 (2006) 011901.

[20] M. Stoica, V. Kolesar, J. Bednarčik, S. Roth, H. Franz, J. Eckert, Journal of Applied Physics 109 (2011) 054901.
[21] P. Pawlik, K. Pawlik, H.A. Davies, J.J. Wysłocki, W. Kaszuwara, M. Leonowicz, Journal of Magnetism and Magnetic Materials 304 (2006) e733.
[22] G.B. Fratucello, P. Vavassori, Journal of Magnetism and Magnetic Materials 260 (2003) 480.
[23] A. Takeuchi, A. Inoue, Materials Transactions 46 (2005) 2817.
[24] E.M. Chudnovsky, Journal of Applied Physics 64 (1988) 5770.
[25] H. Lassri, M. Tlemçani, M. Slimani, S. Sayouri, M. Abid, H. Hamouda, A. Mikou, Physica B 239 (1997) 274.
[26] R. Hasegawa, Journal of Applied Physics 45 (1974) 3109.
[27] G. Herzer, IEEE Transactions on Magnetics 25 (1989) 3327.
[28] N. Heiman, K. Lee, R.I. Potter, S. Kirkpatrick, Journal of Applied Physics 47 (1976) 2634.
[29] J.J. Becker, F.E. Luborsky, J.L. Walter, IEEE Transactions on Magnetics MAG-13 (1977) 988.